biomedicines

MDPI

Article

Augmented Ouabain-Induced Vascular Response Reduces Cardiac Efficiency in Mice with Migraine-Associated Mutation in the Na^+, K^+-ATPase α_2-Isoform

Rajkumar Rajanathan [1,*], Tina Myhre Pedersen [1], Halvor Osterby Guldbrandsen [1], Lenette Foldager Olesen [1], Morten B. Thomsen [2], Hans Erik Bøtker [3] and Vladimir V. Matchkov [1]

[1] Department of Biomedicine, Aarhus University, 8000 Aarhus, Denmark
[2] Department of Biomedical Sciences, University of Copenhagen, 1165 Copenhagen, Denmark
[3] Department of Cardiology, Aarhus University Hospital, 8000 Aarhus, Denmark
* Correspondence: rr@biomed.au.dk

Abstract: Heterozygous mice ($\alpha_2^{+/G301R}$ mice) for the migraine-associated mutation (G301R) in the Na^+,K^+-ATPase α_2-isoform have decreased expression of cardiovascular α_2-isoform. The $\alpha_2^{+/G301R}$ mice exhibit a pro-contractile vascular phenotype associated with decreased left ventricular ejection fraction. However, the integrated functional cardiovascular consequences of this phenotype remain to be addressed in vivo. We hypothesized that the vascular response to α_2-isoform-specific inhibition of the Na^+,K^+-ATPase by ouabain is augmented in $\alpha_2^{+/G301R}$ mice leading to reduced cardiac efficiency. Thus, we aimed to assess the functional contribution of the α_2-isoform to in vivo cardiovascular function of wild-type (WT) and $\alpha_2^{+/G301R}$ mice. Blood pressure, stroke volume, heart rate, total peripheral resistance, arterial dP/dt, and systolic time intervals were assessed in anesthetized WT and $\alpha_2^{+/G301R}$ mice. To address rate-dependent cardiac changes, cardiovascular variables were compared before and after intraperitoneal injection of ouabain (1.5 mg/kg) or vehicle during atrial pacing. The $\alpha_2^{+/G301R}$ mice showed an enhanced ouabain-induced increase in total peripheral resistance associated with reduced efficiency of systolic development compared to WT. When the hearts were paced, ouabain reduced stroke volume in $\alpha_2^{+/G301R}$ mice. In conclusion, the ouabain-induced vascular response was augmented in $\alpha_2^{+/G301R}$ mice with consequent suppression of cardiac function.

Keywords: ouabain; hemodynamic; migraine; cardiovascular function; in vivo; cardiac pacing; total peripheral resistance; Na^+,K^+-ATPase; α_2-isoform

check for updates

Citation: Rajanathan, R.; Pedersen, T.M.; Guldbrandsen, H.O.; Olesen, L.F.; Thomsen, M.B.; Bøtker, H.E.; Matchkov, V.V. Augmented Ouabain-Induced Vascular Response Reduces Cardiac Efficiency in Mice with Migraine-Associated Mutation in the Na^+, K^+-ATPase α_2-Isoform. *Biomedicines* **2023**, *11*, 344. https://doi.org/10.3390/biomedicines11020344

Academic Editors: Elizaveta Klimanova, Olga Lopina and Irina Petrushanko

Received: 13 December 2022
Revised: 22 January 2023
Accepted: 23 January 2023
Published: 25 January 2023

Copyright: © 2023 by the authors. Licensee MDPI, Basel, Switzerland. This article is an open access article distributed under the terms and conditions of the Creative Commons Attribution (CC BY) license (https://creativecommons.org/licenses/by/4.0/).

1. Introduction

Since its discovery in 1957, the Na^+,K^+-ATPase has been extensively studied [1–3]. The Na^+,K^+-ATPase transports three Na^+ ions across the cell membrane to the extracellular milieu, in return, two K^+ ions are transported into the cell [4]. This electrogenic ion transport is crucial for many cellular functions including stabilization of the membrane potential, control of cell volume, and maintaining electrochemical gradients important for the secondary active transport of other ions and substrates across the cell membrane [4]. Recently, the Na^+,K^+-ATPase has also been described to be involved in intracellular signaling [5,6]. The importance of the Na^+,K^+-ATPase is evident by its ubiquitous expression in all eucaryotic cells [7].

The Na^+,K^+-ATPase is a heterodimer transporter that consists of at least an α and a β subunit, and it can also include other regulatory and accessory subunits, e.g., FXYD proteins [8]. The α-subunit is highly conserved across species, and it is responsible for the catalytic and ion-transporting functions of the Na^+,K^+-ATPase [8].

So far, four Na^+,K^+-ATPase α-isoforms have been identified, i.e., the α_1-, α_2-, α_3-, and α_4-isoforms [2,3]. The α-β dimer containing the α_1-isoform is commonly expressed in nearly all cell membranes and is generally thought to have a housekeeping role in controlling transmembrane ion homeostasis [3]. The α_2-isoform is co-expressed with the α_1-isoform in several cell types including muscle tissues, e.g., cardiomyocytes, skeletal, and vascular smooth muscle cells [2,3,9–11].

Changes in the Na^+,K^+-ATPase function are implicated in different pathologies including cardiovascular diseases [2,3,9–15]. In cardiomyocytes and in vascular smooth muscle cells, the Na^+,K^+-ATPase is also important for intracellular Ca^{2+} control and, thus, cardiac and smooth muscle cell contractility [16]. Canonically, the Na^+,K^+-ATPase generates the Na^+ gradient required for the Na^+/Ca^{2+} exchanger to extrude Ca^{2+} [16]. However, the isoform-specificity of this Ca^{2+} regulation has been heavily debated. Moreover, the molecular mechanisms underlying the association between isoform-specific functions and cardiovascular pathology remain unclear [3,17,18].

Familial hemiplegic migraine type 2 (FHM2) is a severe form of inherited migraine with aura [19]. Because FHM2 is associated with mutations in the gene encoding the Na^+,K^+-ATPase α_2-isoform [20], this specific disarray offers an avenue for investigation of the α_2-isoform-specific function in the cardiovascular system. Thus, this study used mice heterozygous for an FHM2-associated mutation (G301R), i.e., ${\alpha_2}^{+/G301R}$ mice [21]. The G301R mutation leads to decreased expression of the Na^+,K^+-ATPase α_2-isoform in both vascular and heart tissues [9–11]. In contrast, the expression of the α_1-isoform is increased in the hearts of ${\alpha_2}^{+/G301R}$ mice [11]. This inverse relationship between the expressions of the α_1- and α_2-isoforms has also been reported for other mouse models [15,22]. The ${\alpha_2}^{+/G301R}$ mouse model is characterized by a changed vascular phenotype [9,10] and an age-dependent (>8 months old) dilation of the ventricles with an associated reduced left ventricular ejection fraction [11].

Cardiac glycosides are a group of molecules that are synthesized by plants and some amphibians [23]. Chemically, they may be characterized by a lactone ring and a steroid ring together with a sugar moiety [23]. The primary mechanism underlying the pharmacodynamics of cardiac glycosides is thought to be their inhibition of the Na^+,K^+-ATPase [23–26]. Cardiac glycosides are known in the clinic for their inotropic and chronotropic properties [27]. However, in research, cardiac glycosides may be used as a tool to characterize the functional contribution of the Na^+,K^+-ATPase to physiological and pathophysiological functions [3,17]. Ouabain is the cardiac glycoside most often used in basic research, and in rodents, ouabain inhibits the isoforms of the Na^+,K^+-ATPase differently in a concentration-dependent manner [3,17,28]. At low concentrations (below 1–10 μM), ouabain inhibits the α_2-isoform and has close to no effect on the α_1-isoform [28]. The α_1-isoform is only inhibited by concentrations that are 100-fold higher due to a genetic variant unique to rodents [8,28]. Consequently, ouabain allows distinction between isoform-specific functions in rodents.

The vascular effects of ouabain are disputed [24–26,29]. While some studies indicate that long-term ouabain administration in rats increases blood pressure in vivo [24,29], other studies suggest no effect of ouabain on blood pressure [25,26]. Additionally, ex vivo studies suggest both ouabain-induced impairment and augmentation of vascular contractility depending on the vascular bed [24,26,30]. This matter is further complicated in vivo due to the inotropic effects of ouabain, which may also contribute to alterations in blood pressure [31,32]. Whether the conflicting data are due to variations in the inhibition of isoform-specific functions of the Na^+,K^+-ATPase remains unknown. The integrated cardiovascular assessment in vivo may be helpful in distinguishing between the cardiac and vascular components of the effect of ouabain and α_2-isoform function. We have previously validated an experimental setup that allows for: (i) Comprehensive assessment of cardiac and vascular functions; (ii) control of heart rate through atrial pacing and examination of rate-dependent variables; and (iii) distinction between simultaneous changes in cardiac and vascular variables in vivo in the anesthetized mouse [33]. Therefore, in this study, we aimed

to comprehensively characterize the cardiovascular effect of ouabain in aged (>8 months old) $\alpha_2^{+/G301R}$ mice, which were previously shown to have reduced left ventricular ejection fraction [11], and to compare cardiac and vascular responses to ouabain in $\alpha_2^{+/G301R}$ mice and matching wild-type mice (WT).

We hypothesized that the effect of ouabain on cardiac and vascular functions is greater in $\alpha_2^{+/G301R}$ mice compared to WT at plasma ouabain concentrations inhibiting the α_2-isoform. This is due to the reduced expression of the α_2-isoform in the cardiovascular system of $\alpha_2^{+/G301R}$ mice resulting in a more efficient ouabain-induced inhibition compared to that of the WT.

Our study demonstrates the importance of Na^+,K^+-ATPase α_2-isoform for vascular function and links the ouabain-responsive vascular phenotype in $\alpha_2^{+/G301R}$ mice to consequences for their cardiac function in vivo.

2. Materials and Methods

2.1. Experimental Animals

According to the cardiac phenotype previously described in aged $\alpha_2^{+/G301R}$ mice [11], we used aged $\alpha_2^{+/G301R}$ and WT mice with C57BL/6J background (>8 months old) in this study. Investigators were blinded regarding the genotype of animals. The $\alpha_2^{+/G301R}$ mouse line was generated as previously described [21], and they were kept and bred at Aarhus University, Denmark. The homozygous genotype for the G301R mutation is lethal, therefore, only heterozygous mice were available for this study [34,35]. No sex differences have previously been observed in the cardiovascular phenotype of $\alpha_2^{+/G301R}$ mice [9–11]. Thus, due to their larger body sizes, only male mice (n = 12 for $\alpha_2^{+/G301R}$ and n = 12 for WT) were used in this study. Our approach yielded a higher surgical success rate ultimately reducing the number of animals used.

Mice were housed in rooms with controlled temperature (21.5 °C) and humidity (55%) with a 12:12 h light-dark cycle. Mice had ad libitum access to food and water. All animal experiments conformed to the guidelines from Directive 2010/63/EU of the European Parliament on the protection of animals used for scientific purposes. The experimental protocol was approved by the Animal Experiments Inspectorate of the Danish Ministry of Environment and Food and reported in accordance with the ARRIVE (Animal Research: Reporting in vivo Experiments) guidelines [36]. Mice were euthanized under deep anesthesia by cervical dislocation at the end of the study.

2.2. In Vivo Cardiovascular Study

The surgical preparation of mice and implantation of catheter, probe, and electrodes were done as previously described [33]. Mouse core temperature was kept at 37 ± 0.5 °C with a homeothermic blanket system (50-7222F, Harvard Apparatus, Holliston, MA, USA). Mice were mechanically ventilated with a MiniVent Ventilator (model 845, Harvard Apparatus, Holliston, MA, USA) under isoflurane anesthesia (induced at 3% and maintained at 2% in 100% O_2 throughout the experiment). Ventilation was connected to a capnograph (Type 340, Harvard Apparatus, Holliston, MA, USA) relaying end-tidal CO_2 ($\%_{et}CO_2$). Tidal volume relied on body mass (10 µL/g) [37]. Respiration rate was adjusted according to $\%_{et}CO_2$ (approximately 3.5%) [38], and it was then kept constant. For arterial blood pressure measurements, the tip of a 1.0 F solid-state catheter (SPR-1000, Millar, Houston, TX, USA) was introduced into the right common carotid artery and placed in the aortic arc. A transit-time flow probe (1.5 SL, Transonic, Ithaca, NY, USA) soaked in ultrasound gel (Kruuse, Langeskov, Denmark) was latched onto the ascending aorta. Flow measured by this flow probe was used as a proxy for cardiac output. Platinum bipolar electrodes positioned on the sinus node were used for electrical atrial pacing and were connected to a dual bioamplifier/stimulator unit (ADInstruments, Sydney, Australia). The electrical pulse width and the current used were 0.2 ms and 3 mA, respectively. Electrocardiogram (ECG) leads I and II were recorded with electrodes on the paws (MLA2505, ADInstruments, Sydney, Australia). During surgical preparation, mice were subject to intraperitoneal (i.p.)

administration of pancuronium-bromide (0.4 mg/kg; P1918, Sigma, St. Louis, MO, USA) for the inhibition of respiratory reflexes and NaCl solution (1 mL, 9 mg/mL NaCl; Fresenius Kabi, Bad Homburg, Germany) to compensate any fluid loss.

Instrumentation of the flow probe and blood pressure catheter was successful in all 24 mice. However, the ECG recording of one WT mouse in the vehicle group was not interpretable. Thus, systolic time intervals were not calculated for this mouse.

Following stabilization of cardiovascular variables under the set respiratory parameters, the protocol was initiated (Figure 1). The protocol consisted of two rounds of atrial pacing with administration of either ouabain (1.5 mg/kg i.p., Sigma, St. Louis, MO, USA) or a corresponding volume of vehicle (9 mg/mL i.p., NaCl). First, to control heart rate, atrial pacing was done at 10 Hz with stepwise increments to 11.3 Hz (678 BPM) and then kept for 20 s as previously described [33]. Then, after one minute of sinus rhythm, i.e., heart rate without atrial pacing, ouabain or vehicle was administered i.p., and 5 min were given for cardiovascular variables to restabilize. Eight animals from each genotype were randomized to ouabain administration, and four animals from each genotype were randomized to vehicle administration. Another atrial pacing session was performed at 10 Hz with stepwise increments to 11.3 Hz, which was also kept for 20 s. Subsequently, the protocol was finalized with 6 min of sinus rhythm.

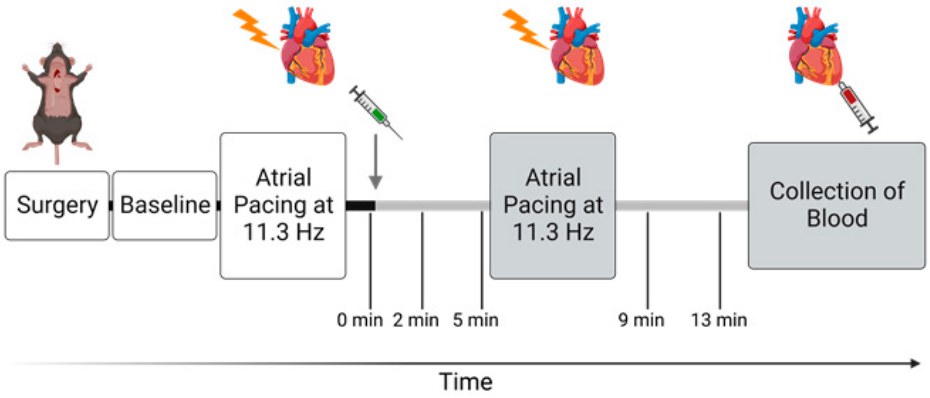


Figure 1. Timeline of the in vivo protocol. Gray arrow indicates point of intraperitoneal injection of either ouabain (1.5 mg/kg) or vehicle (0.9 mg/mL NaCl), and gray bars indicate period after administration. After implantation of probes, a baseline measurement was made. The protocol includes atrial pacing starting from 10 Hz (600 BPM) with stepwise increments to 11.3 Hz (678 BPM) before and after administration. Time points 0, 2, 5, 9, and 13 min represent measurements done during sinus rhythm. The protocol was finalized by blood collection from the apex 15 min after administration of ouabain or saline. Figure was created with BioRender.com.

At the end of the experiment, which was approximately 15 min after i.p. injection, blood was collected from the left ventricle in heparinized Eppendorf tubes. The whole blood was centrifuged in a Biofuge centrifuge (Biofuge Fresco, Heraeus, Hanau, Germany) at 2000 RPM (g-force of approximately 310 m/s^2) and 4 °C for 10 min to separate the blood components. Plasma was collected and snap-frozen for plasma ouabain analysis. This included 4 and 5 samples in the vehicle groups together with 7 and 13 samples in the ouabain groups for $\alpha_2^{+/G301R}$ and WT mice, respectively.

2.3. Measurements of Plasma Ouabain Concentration

Plasma ouabain concentrations were measured with an ELISA kit (CEV857Ge, Cloud-Clone Corp., Houston, TX, USA). The assay was prepared according to the manufacturer's instructions. To increase the detection range for the standard ouabain concentration curve, we utilized the linearity of the standard ouabain concentration curve in ouabain concentration range of 50,000, 16,666.7, 5555.6, 1851.9, 617.3, 205.7, and 68.60 pg/mL. Each sample measurement was duplicated. The experiment and analysis were performed in a blinded fashion. The signal optical density was measured in a microplate spectrophotometer (Powerwave 340, BioTek, Winooski, VT, USA).

2.4. Data Acquisition and Calculations

All data were recorded in LabChart Pro 8 (ADInstruments, Sydney, Australia). Hemodynamic and ventilation variables were acquired at a sampling rate of 1 kHz using a Powerlab unit (PowerLab 16/35, ADInstruments, Sydney, Australia). The mouse ECG lead I and II were recorded with a sampling rate of 4 kHz. Hemodynamic variables were averaged over one minute. During atrial pacing, variables were averaged over a period of 20 s. Blood flow was measured as the integral of the transit-time flow measurement [39], and cardiac output was calculated based on the measured time interval. Stroke volume was calculated from heart rate and cardiac output. Total peripheral resistance was calculated from mean arterial pressure and cardiac output [40]. As indices for contractility and efficiency of relaxation, the maximum positive first-time derivative (dP/dt_{max}) [41] and the minimum negative first-time derivative (dP/dt_{min}) [42] were calculated based on arterial blood pressure measurements, respectively. The systolic time intervals were calculated to estimate myocardial efficiency [43]. This was done based on the temporal relationship between the QRS complex from lead I of the mouse ECG and the opening and closure of the aortic valve based on the blood pressure waveform and blood flow trace (Figure 2). For calculating the systolic time intervals, a script developed in MatLab (MatLab R2020a, MathWorks, Natick, MA, USA) was used. The pre-ejection period was defined as the time between the start of the QRS complex and the opening of the aortic valve indicated by the initial peak of blood flow acceleration in the aorta [44,45]. Left ventricular ejection time was defined as the time between opening of the aortic valve until its closure indicated by the dicrotic notch on the blood pressure waveform [44,46]. The systolic time interval ratio was calculated by dividing pre-ejection period by left ventricular ejection time [43]. Systolic duration was defined as the sum of the pre-ejection period and left ventricular ejection time.

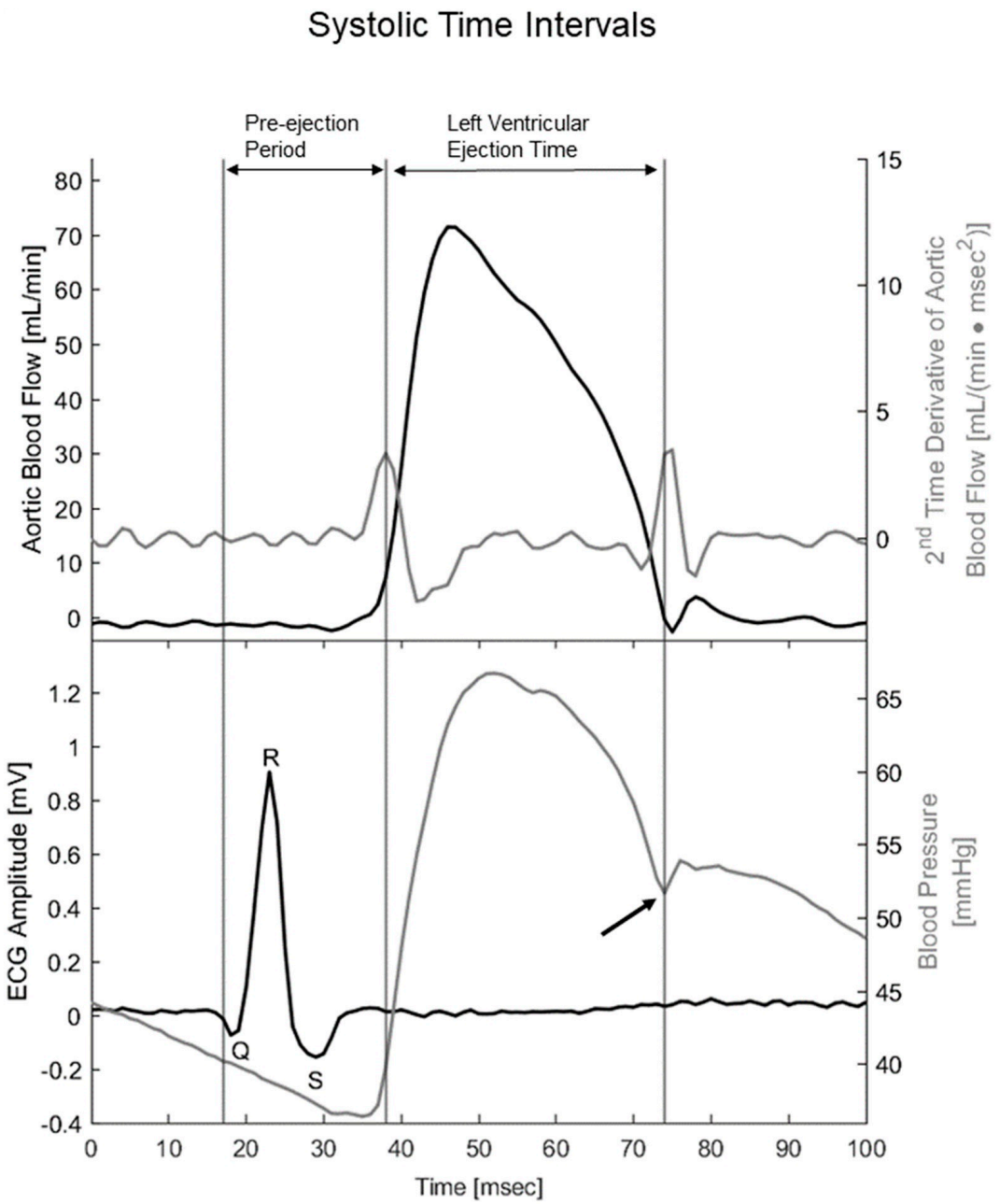


Figure 2. Temporal alignment between the second time derivative of aortic blood flow, ECG, and blood pressure traces allowed for the calculation of systolic time intervals. Upper panel includes blood flow through the ascending aorta (black line) and its 2nd time derivative, i.e., acceleration (gray line). Lower panel includes mouse ECG lead I with depicted Q, R, and S waves (black line) together with arterial blood pressure measured in the aortic arc (gray line). Black arrow indicates the dicrotic notch on the blood pressure trace, i.e., closure of the aortic valve. Preejection period was defined as spanning from the beginning of the Q wave to opening of the aortic valve, i.e., Q wave to the first peak of the second time derivative of aortic flow. Left ventricular ejection period was defined as spanning from the opening to the closure of the aortic valve, i.e., spanning from the first peak of the second time derivative of blood flow to the dicrotic notch. Systolic duration was defined as the sum of the pre-ejection period and left ventricular ejection time.

2.5. Statistical Analysis

All data are presented as mean values ± SEM. Also, pacing data are presented as mean values with individual paired data points. If data violated the assumption of nor-

mality, a non-parametric test was used for analysis as indicated. Baseline parameters and cardiovascular variables were compared with an unpaired *t*-test or a Mann–Whitney test. In vivo functional data were analyzed with multiple Wilcoxon tests or a two-way repeated measures ANOVA. Dunnett's or Bonferroni's multiple comparison tests were used when a statistically significant effect of a variable was detected. Plasma ouabain concentrations were analyzed with a two-way ANOVA followed by Bonferroni's multiple comparison test. *p*-values below 0.05 were considered statistically significant.

3. Results

3.1. Baseline Physiological Variables Were Similar between WT and $\alpha_2^{+/G301R}$ Mice

All mice were of the same age and displayed similar body mass. The physiological variables assessed before atrial pacing and pharmacological intervention were also similar between anesthetized WT and $\alpha_2^{+/G301R}$ mice (Table 1).

Table 1. Baseline in vivo parameters and cardiovascular variables of all wild-type and $\alpha_2^{+/G301R}$ mice were similar. One wild-type mouse injected with vehicle had an uninterpretable ECG recording and, thus, was excluded in systolic time interval calculations. Data were compared with an unpaired *t*-test or a Mann–Whitney test where appropriate.

	Wild Type (n = 12)	**$\alpha_2^{+/G301R}$ (n = 12)**	***p*-Value**
Age (weeks)	41 ± 2	45 ± 3	0.23
Body mass (g)	35.3 ± 1.6	35.3 ± 0.8	>0.99
Cardiovascular variables and respiratory parameters			
Systolic pressure (mmHg)	76.09 ± 2.97	72.09 ± 4.68	0.48
Diastolic pressure (mmHg)	49.71 ± 3.53	46.16 ± 5.00	0.57
Total peripheral resistance (mmHg•min/mL)	6.89 ± 0.71	7.21 ± 0.73	0.76
Cardiac output (mL/min)	9.13 ± 0.75	8.28 ± 0.93	0.48
Stroke volume (µL)	17.20 ± 1.50	15.66 ± 1.83	0.52
Heart rate (BPM)	534 ± 8	530 ± 10	0.81
End-tidal CO_2 (%)	3.69 ± 0.13	3.76 ± 0.11	0.69
Ventilation rate (min^{-1})	116 ± 6	114 ± 7	0.87
Systolic time interval ratio (AU.)	0.59 ± 0.04	0.54 ± 0.03	0.27
Pre-ejection period (ms)	19.2 ± 0.8	18.2 ± 0.5	0.28
Left ventricular ejection time (ms)	33.2 ± 1.5	34.4 ± 1.6	0.58
Systolic duration (ms)	52.4 ± 1.6	52.6 ± 1.8	0.82
Arterial dP/dt_{max} (mmHg/s)	3705 ± 298.9	3142 ± 197.9	0.13
Arterial dP/dt_{min} (mmHg/s)	−2157 ± 92.78	−2106 ± 134.4	0.76

3.2. Administration of Ouabain Similarly Elevates the Plasma Ouabain Concentrations in WT and $\alpha_2^{+/G301R}$ Mice

Injection of ouabain (1.5 mg/kg, i.p.,) significantly increased plasma ouabain concentrations of both WT and $\alpha_2^{+/G301R}$ mice ($p < 0.0001$; Figure 3). There was no genotype effect in plasma ouabain concentrations before and after interventions (Figure 3).

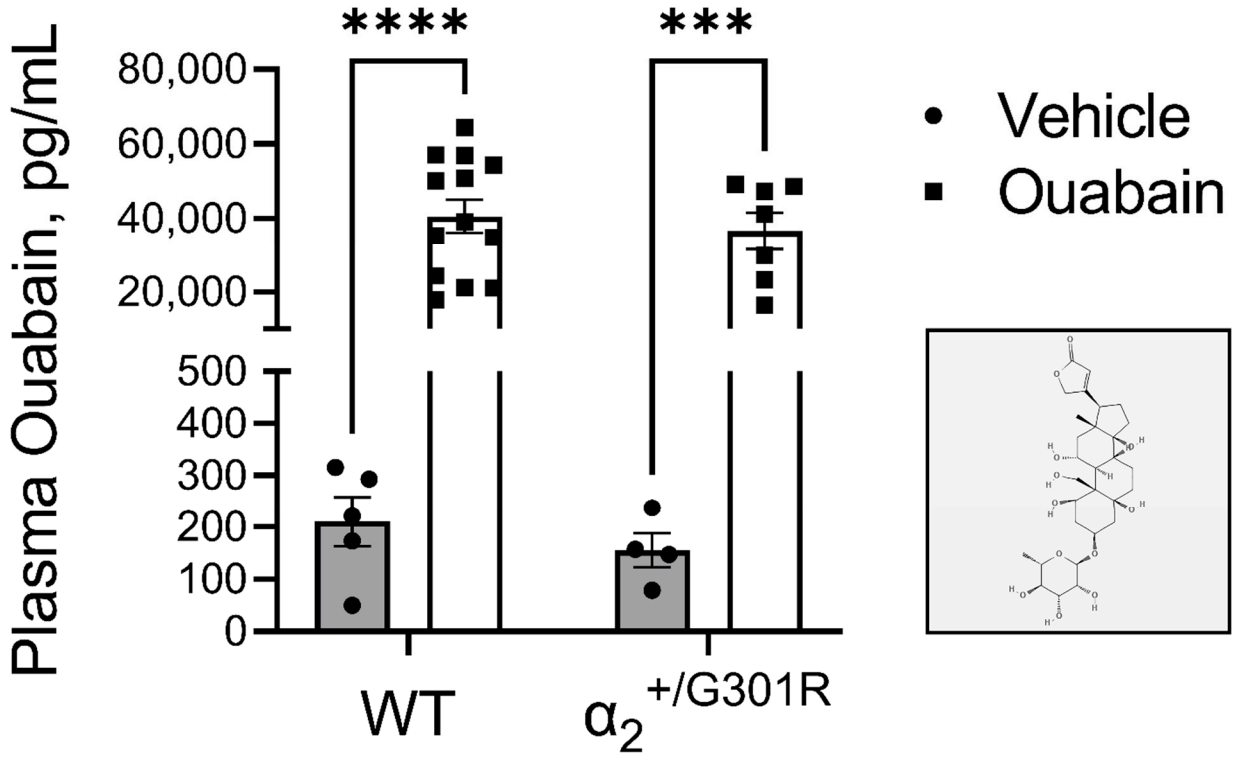


Figure 3. Similar plasma ouabain concentrations between wild-type (WT) and $\alpha_2^{+/G301R}$ mice approximately 15 mins after injection of ouabain (1.5 mg/kg) or vehicle (0.9% NaCl) treatment. Injection of ouabain i.p. increased plasma ouabain concentrations similarly in both WT (210 ± 48 pg/mL and 40,517 ± 4438 pg/mL for vehicle and ouabain administered mice, respectively) and $\alpha_2^{+/G301R}$ (156 ± 33 pg/mL and 36,489 ± 5041 pg/mL for vehicle and ouabain administered mice, respectively) mice compared to their respective vehicle groups. (Insert) The molecular structure of ouabain in 2D (adopted from the PubChem database [47]). ELISA data were analyzed by two-way ANOVA followed by Bonferroni's multiple comparison test. *** $p = 0.0003$ and **** $p < 0.0001$; intragroup plasma ouabain concentration of vehicle vs. ouabain treated mice. $n = 7$–13 for ouabain groups, and $n = 4$–5 for vehicle groups.

3.3. Ouabain Elevated Peripheral Vascular Resistance and Blood Pressure While Cardiac Variables Were Unchanged in Both WT and $\alpha_2^{+/G301R}$ Mice

In general, ouabain administration increased systolic blood pressure ($p = 0.0193$); however, following post-hoc analysis, the changes in WT systolic pressure did not achieve statistical significance ($p = 0.0993$, $p = 0.0901$, $p = 0.0556$, and $p = 0.0944$ for 2, 5, 9, and 13 min, respectively, after ouabain administration compared to the time prior injection; Figure 4a). The diastolic blood pressure was increased in both genotypes ($p = 0.0100$; Figure 4a). The increase in blood pressure was associated with ouabain-induced elevation in total peripheral resistance ($p < 0.0001$). The dynamic of these changes was steeper in $\alpha_2^{+/G301R}$ mice than in WT mice ($p = 0.0340$; Figure 4b). Ouabain administration did not modify stroke volume, heart rate, or cardiac output (Figure 4c–e).

Ouabain administration significantly increased the systolic time interval ratio of $\alpha_2^{+/G301R}$ mice only ($p = 0.0004$; Figure 5a). This was associated with ouabain-induced prolongation of the pre-ejection period ($p = 0.0007$) and shortening of the left ventricular ejection time ($p = 0.0426$; Figure 5b,c). Systolic time intervals of WT mice were unchanged. The systolic duration, arterial dP/dt_{max}, and arterial dP/dt_{min} were not affected by ouabain administration in both $\alpha_2^{+/G301R}$ and WT mice (Figure 5d–f).

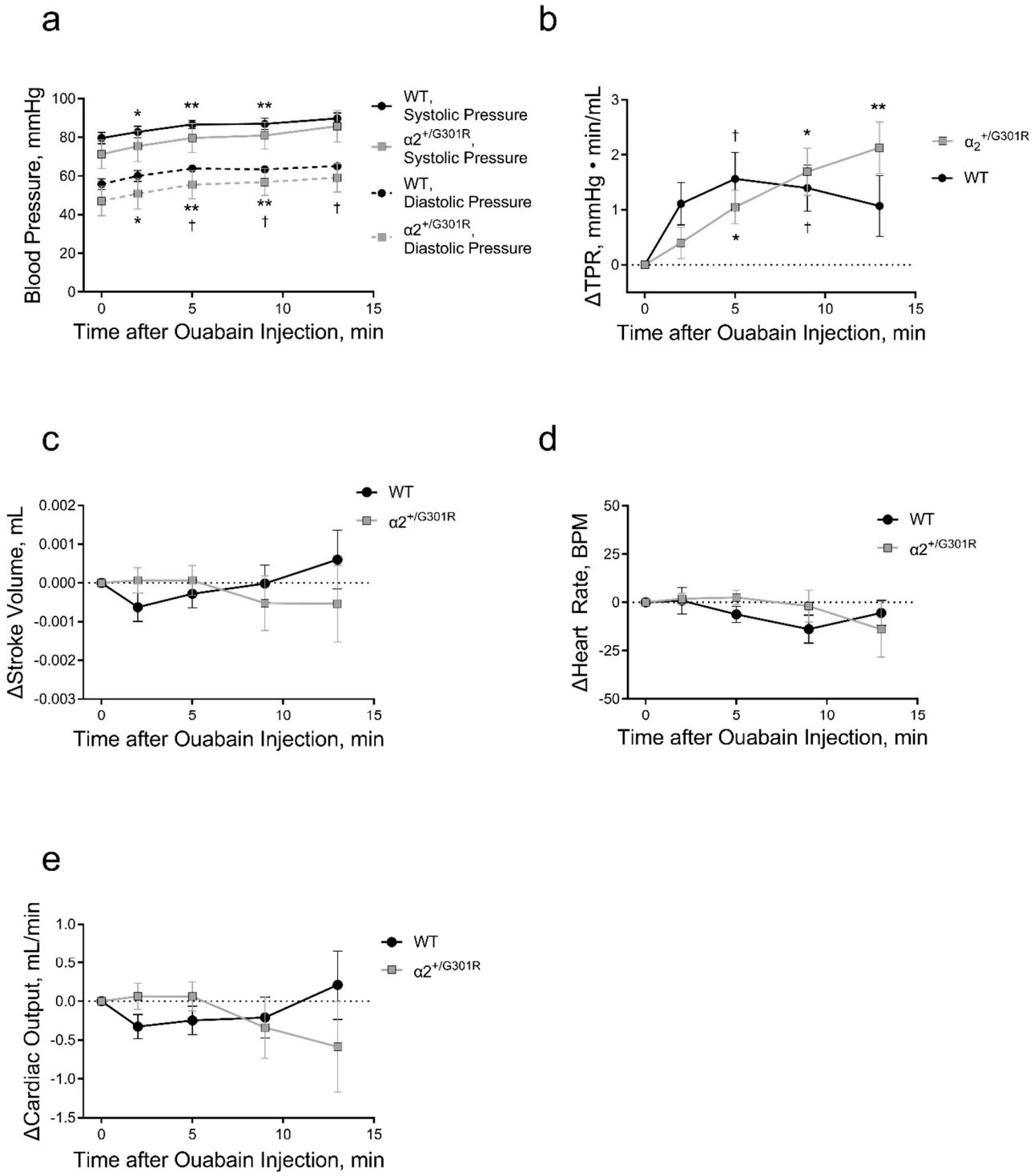


Figure 4. Intraperitoneal ouabain injection (1.5 mg/kg) increased blood pressure and total peripheral resistance in wild-type (WT) and $\alpha_2^{+/G301R}$ mice. (**a**) Ouabain increased blood pressure in WT and $\alpha_2^{+/G301R}$ mice (systolic pressure; $p = 0.0193$, and diastolic pressure; $p = 0.0100$). (**b**) Ouabain-induced increase in total peripheral resistance (TPR) was different between $\alpha_2^{+/G301R}$ and WT mice ($p = 0.0340$). There was no significant effect of ouabain administration on stroke volume (**c**), heart rate (**d**), or cardiac output (**e**) in neither WT nor $\alpha_2^{+/G301R}$ mice. Data were compared with two-way repeated measures ANOVA followed by Dunnett's multiple comparison test. * $p < 0.05$ and ** $p < 0.01$ for $\alpha_2^{+/G301R}$ and † $p < 0.05$ for WT; variables at different time points vs. intragroup baseline before ouabain administration, i.e., time 0 min. $n = 8$. Data are available in Supplementary Table S1.

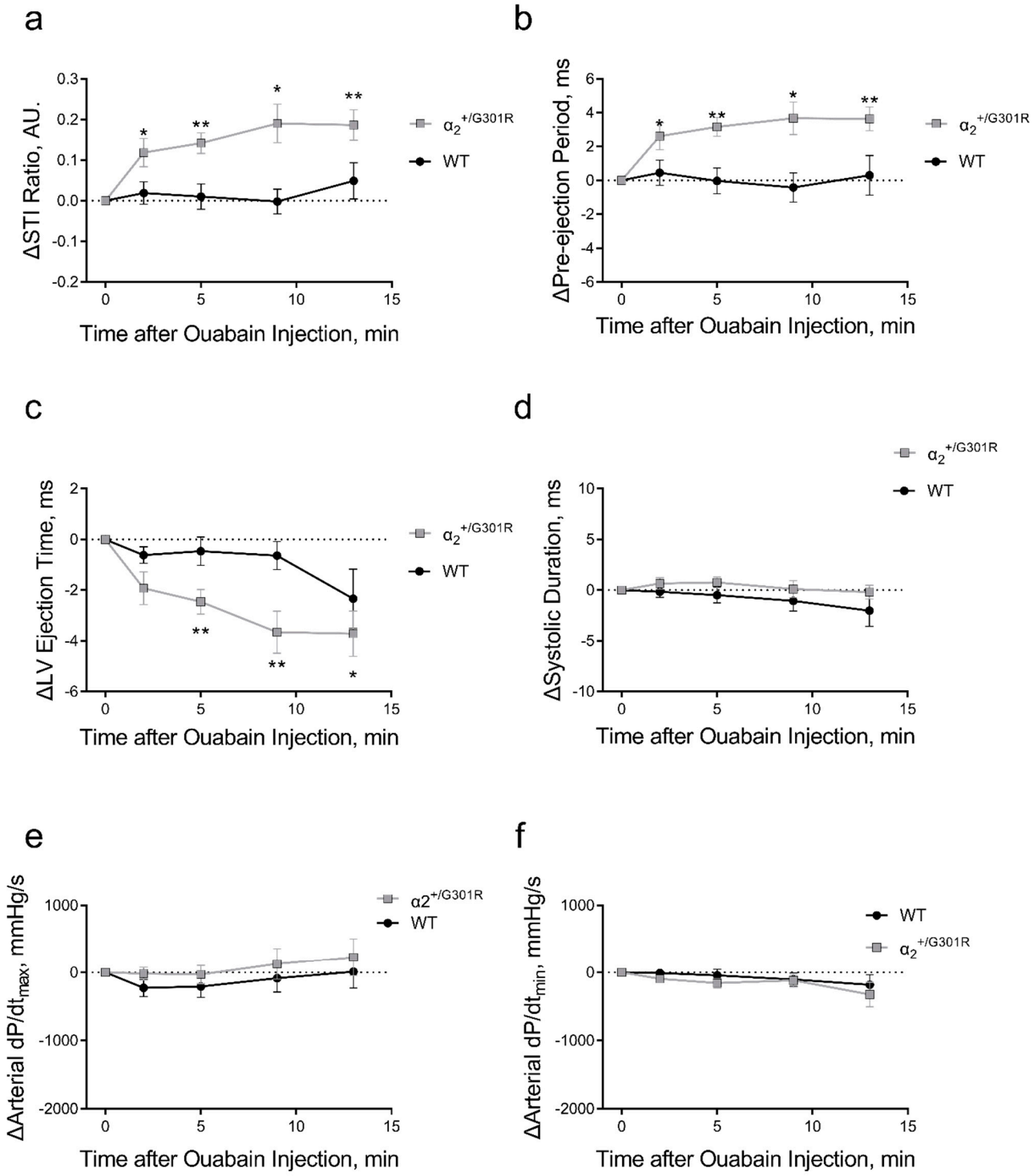


Figure 5. Systolic time intervals were affected by ouabain administration (1.5 mg/kg, i.p.) only in $\alpha_2^{+/G301R}$ mice and not in wild-type mice (WT). (**a**) the systolic time interval ratio (STI Ratio) was significantly increased in $\alpha_2^{+/G301R}$ mice only ($p = 0.0004$) due to (**b**) prolongation of pre-ejection period ($p = 0.0007$) and (**c**) shortening of left ventricular ejection time (LV Ejection Time; $p = 0.0426$). (**d**) Systolic duration, (**e**) arterial dP/dt_{max}, and (**f**) arterial dP/dt_{min} were unchanged in both WT and $\alpha_2^{+/G301R}$ mice after ouabain administration. Data were compared with two-way repeated measures ANOVA followed by Dunnett's multiple comparison test. * $p < 0.05$ and ** $p < 0.01$ for $\alpha_2^{+/G301R}$; variables at different time points vs. intragroup baseline before ouabain administration, i.e., time 0 min. $n = 8$. Data are available in Supplementary Table S1.

Vehicle administration had no effect on blood pressure, total peripheral resistance, stroke volume, heart rate, nor cardiac output in both $\alpha_2^{+/G301R}$ and WT mice (Supplementary Figure S1). Similarly, no effect of vehicle administration was observed in systolic time intervals nor in systolic duration, arterial dP/dt_{max}, and arterial dP/dt_{min} (Supplementary Figure S2).

3.4. When Heart Rate Was Controlled, Ouabain Administration Reduced Stroke Volume in $\alpha_2^{+/G301R}$ Mice

When heart rate was kept at 11.3 Hz (678 BPM) by atrial pacing, ouabain administration significantly increased both systolic ($p = 0.0002$) and diastolic blood pressure ($p < 0.0001$) in both $\alpha_2^{+/G301R}$ and WT mice (Figure 6a,b). This increase in blood pressure was accompanied with an ouabain-induced augmentation of total peripheral resistance in both genotypes ($p = 0.0001$; Figure 6c).

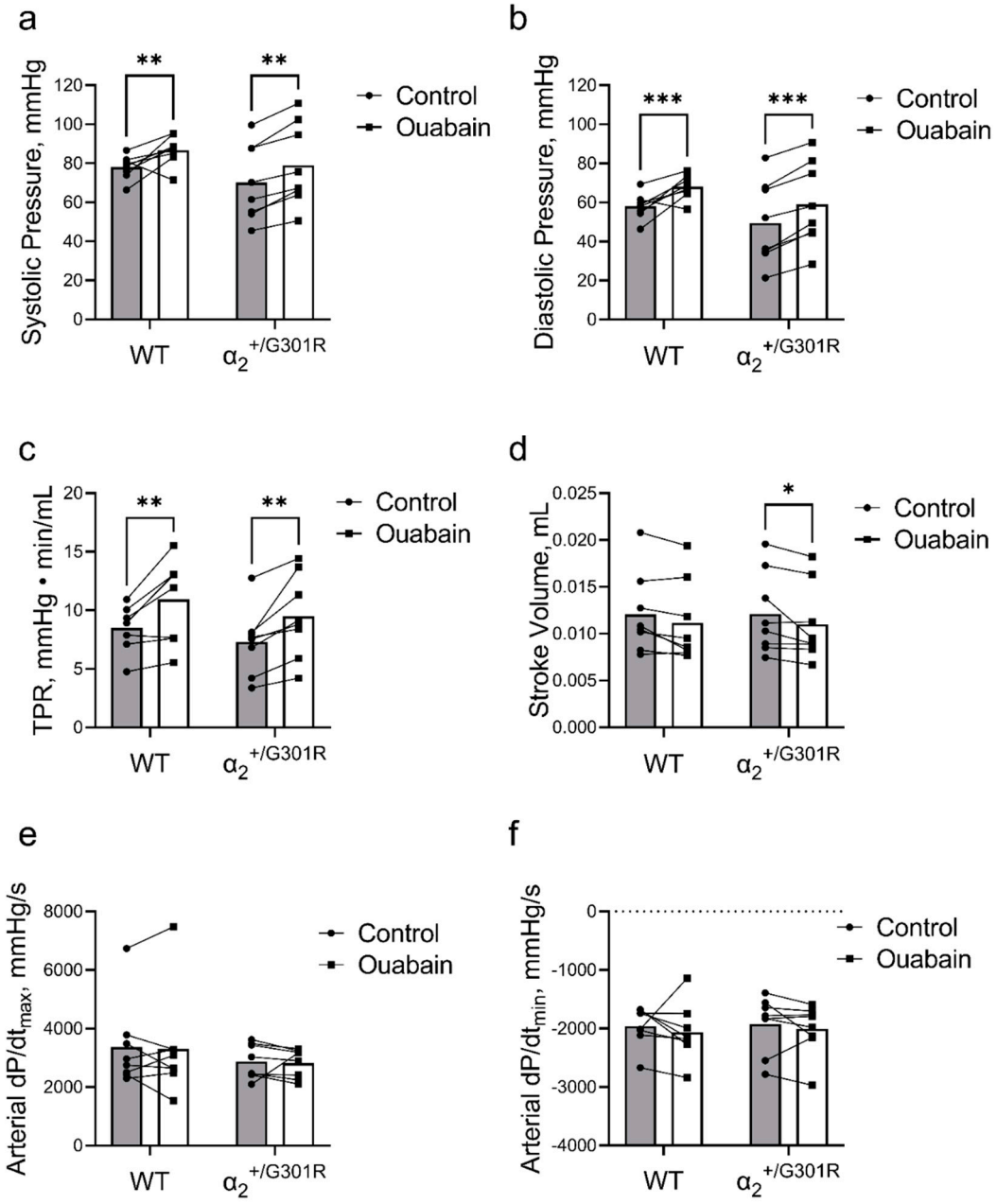


Figure 6. Ouabain administration increased blood pressure and total peripheral resistance in both wild-type (WT) and $\alpha_2^{+/G301R}$ mice when the hearts were paced at 11.3 Hz (678 BPM). Under these

conditions, ouabain reduced stroke volume in $\alpha_2^{+/G301R}$ mice. Administration of ouabain augmented (**a**) systolic blood pressure (control vs. ouabain; 78.01 ± 2.14 mmHg vs. 86.71 ± 2.67 mmHg for WT and 70.19 ± 6.90 mmHg vs. 78.94 ± 7.50 mmHg for $\alpha_2^{+/G301R}$ mice; $p = 0.0002$), (**b**) diastolic blood pressure (control vs. ouabain; 58.01 ± 2.31 mmHg vs. 68.01 ± 2.16 mmHg for WT and 49.50 ± 7.51 mmHg vs. 59.03 ± 7.56 mmHg for $\alpha_2^{+/G301R}$ mice; $p < 0.0001$), and (**c**) total peripheral resistance (TPR; control vs. ouabain; 8.49 ± 0.68 mmHg·min/mL vs. 10.92 ± 1.24 mmHg·min/mL for WT and 7.31 ± 1.00 mmHg·min/mL vs. 9.48 ± 1.25 mmHg·min/mL for $\alpha_2^{+/G301R}$ mice; $p = 0.0001$). Ouabain administration significantly decreased stroke volume (**d**) in $\alpha_2^{+/G301R}$ mice (control vs. ouabain; 12.12 ± 1.54 µL vs. 11.02 ± 1.45 µL; $p = 0.0473$), whereas changes to stroke volume in WT mice did not achieve statistical significance (control vs. ouabain; 12.07 ± 1.53 µL vs. 11.15 ± 1.54 µL; $p = 0.1062$). (**e**) Arterial dP/dt_{max} (control vs. ouabain; 3367 ± 516 mmHg/s vs. 3303 ± 629 mmHg/s for WT and 2872 ± 209 mmHg/s vs. 2820 ± 174 mmHg/s for $\alpha_2^{+/G301R}$ mice) and (**f**) arterial dP/dt_{min} (control vs. ouabain; −1958 ± 119 mmHg/s vs. −2067 ± 172 mmHg/s for WT and −1922 ± 172 mmHg/s vs. −2009 ± 155 mmHg/s for $\alpha_2^{+/G301R}$ mice) were unchanged in both groups. Data were compared with multiple Wilcoxon tests or two-way repeated measures ANOVA followed by Bonferroni's multiple comparison test. * $p < 0.05$, ** $p < 0.01$, and *** $p < 0.001$; intragroup variables before vs. after ouabain administration. $n = 8$.

A general effect of ouabain on stroke volume was detected during atrial pacing ($p = 0.0054$); however, following post-hoc analysis, ouabain administration reduced stroke volume during atrial pacing at 11.3 Hz in $\alpha_2^{+/G301R}$ mice ($p = 0.0473$), whereas the change in stroke volume in WT did not achieve statistical significance ($p = 0.1062$; Figure 6d).

Arterial dP/dt_{max} and arterial dP/dt_{min} were unchanged after ouabain administration during atrial pacing in both groups (Figure 6e,f).

Blood pressure, total peripheral resistance, and stroke volume were unaffected by vehicle injection in both groups during atrial pacing at 11.3 Hz (Supplementary Figure S3a–d). However, when the hearts were paced at 11.3 Hz, arterial dP/dt_{max} was greater in WT mice compared to $\alpha_2^{+/G301R}$ mice after vehicle administration ($p = 0.0192$; Supplementary Figure S3e). There was no change to arterial dP/dt_{min} (Supplementary Figure S3f).

3.5. When Heart Rate Was Controlled at 11.3 Hz, Ouabain-Induced Changes to Systolic Time Intervals in $\alpha_2^{+/G301R}$ Mice Were Abolished

When the hearts were paced at 11.3 Hz, variables related to systolic time intervals including the systolic time interval ratio, pre-ejection period, left ventricular ejection time, and systolic duration were similar between genotypes before and after ouabain administration (Figure 7). Similarly, the systolic time interval ratio, pre-ejection period, left ventricular ejection time, and systolic duration were not affected by vehicle injection when the hearts were paced at 11.3 Hz (Supplementary Figure S4).

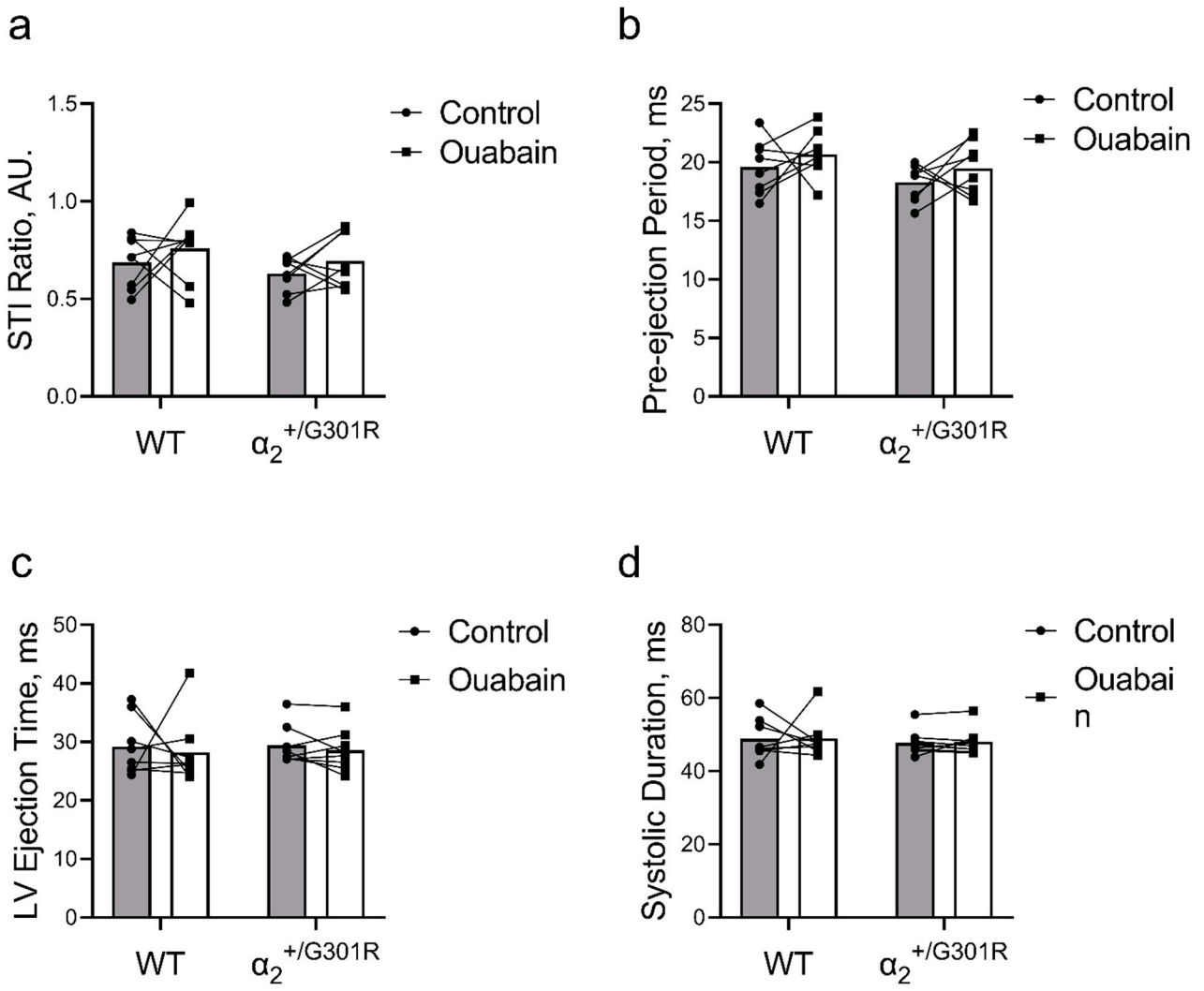


Figure 7. Ouabain administration was without an effect on systolic time intervals in $\alpha_2^{+/G301R}$ and wild-type mice (WT) when the hearts were paced at 11.3 Hz (678 BPM). (**a**) The systolic time interval ratio (STI Ratio; control vs. ouabain; 0.69 ± 0.04 vs. 0.76 ± 0.06 for WT and 0.63 ± 0.03 vs. 0.69 ± 0.05 for $\alpha_2^{+/G301R}$ mice), (**b**) pre-ejection period (control vs. ouabain; 19.6 ± 0.8 ms vs. 20.7 ± 0.7 ms for WT and 18.3 ± 0.5 ms vs. 19.5 ± 0.8 ms for $\alpha_2^{+/G301R}$ mice), (**c**) left ventricular ejection time (LV ejection time; control vs. ouabain; 29.2 ± 1.8 ms vs. 28.2 ± 2.1 ms for WT and 29.4 ± 1.2 ms vs. 28.6 ± 1.3 ms for $\alpha_2^{+/G301R}$ mice), and (**d**) systolic duration (control vs. ouabain; 48.8 ± 2.0 ms vs. 49.0 ± 1.9 ms for WT and 47.7 ± 1.2 ms vs. 48.1 ± 1.3 ms for $\alpha_2^{+/G301R}$ mice) were similar during atrial pacing at 11.3 Hz before and after ouabain administration. Data were compared with two-way repeated measures ANOVA. n = 8.

4. Discussion

We aimed to characterize the Na^+,K^+-ATPase α_2-isoform-specific contribution to cardiovascular function and, thus, investigated the comprehensive cardiovascular responses to ouabain of $\alpha_2^{+/G301R}$ and WT mice. Additionally, we paced the hearts to discern potential rate-dependent changes to cardiac function associated to ouabain or the phenotype of the $\alpha_2^{+/G301R}$ mouse model [48,49].

We hypothesized that the cardiovascular response to ouabain in $\alpha_2^{+/G301R}$ mice was augmented due to their reduced expression of the Na^+,K^+-ATPase α_2-isoform compared to WT. Pharmacologically, at a specific drug concentration, the effect of a drug may be described by how many receptors it binds relative to the total amount of receptors expressed on the cell membrane, i.e., fractional occupancy [50]. Mathematically, fractional occupancy

equals the occupied binding sites divided by the number of total binding sites [50]. Thus, the fewer α_2-isoforms present in the cell membrane of $\alpha_2^{+/G301R}$ mice results in higher fractional occupancy and effect of a specific concentration of ouabain [9,11].

Accordingly, we found that the peripheral vascular effect of ouabain in vivo was augmented in the $\alpha_2^{+/G301R}$ mice compared to WT. This was associated with ouabain-induced changes in the temporal development of the systole in $\alpha_2^{+/G301R}$ mice. However, stroke volume remained unchanged during sinus rhythm in $\alpha_2^{+/G301R}$ mice despite an increased total peripheral resistance and change in systolic function. Even so, stroke volume was reduced in $\alpha_2^{+/G301R}$ mice during atrial pacing after ouabain administration. Thus, in this study we demonstrated an association between the ouabain-sensitive vascular phenotype in $\alpha_2^{+/G301R}$ mice with reduced cardiac efficiency.

Different ouabain-sensitivity of the α_1- and α_2-isoforms of Na^+,K^+-ATPase in rodents [8] allows isoform-specific differentiation of their functions in the cardiovascular system [51]. The isoform-specific half-maximal inhibitory concentrations, i.e., IC50, of ouabain were reported to be 48,000 nM and 58 nM for the α_1- and α_2-isoforms in rats, respectively [28]. In our study, the basal plasma level of endogenous ouabain and its concentration after injection of exogenous ouabain were similar between $\alpha_2^{+/G301R}$ and WT mice. We estimated that the basal concentration of ouabain in mouse plasma was approximately 300 pM. This concentration is in close agreement with previously reported concentrations for rodents and humans [52,53]. Furthermore, in this study, injection of exogenous ouabain elevated the plasma ouabain concentration to approximately 100 nM, i.e., a concentration that affects the α_2-isoform and not the α_1-isoform function. In our preliminary study, higher concentrations of ouabain were lethal presumably due to complete inhibition of the Na^+,K^+-ATPase emphasizing the vital importance of the Na^+,K^+-ATPase function for living cells. Furthermore, the Na^+,K^+-ATPase α_3-isoform is mostly allocated to neuronal tissues [2], and the blood–brain barrier is not permeable to circulating ouabain [54]. Therefore, we anticipated that the cardiovascular α_2-isoform was the primary target of the pharmacological intervention in this study. However, we cannot exclude that some of the effects of ouabain administration were mediated via the autonomic nervous system [55].

In our earlier study, we found that during nighttime, i.e., the active period of mouse circadian rhythm, aged (>8 months old) $\alpha_2^{+/G301R}$ mice exhibited reduced blood pressure compared to WT [11]. However, blood pressure during daytime, i.e., the inactive period of mouse circadian rhythm, was the same between the two genotypes [11]. Accordingly, no difference in blood pressure between genotypes was seen in this study in anesthetized mice under baseline conditions.

In accordance with previous reports on rodents, we found that ouabain administration increased blood pressure [29,56]. The ouabain-induced blood pressure elevation has previously been ascribed to the inotropic effect of ouabain [31,32]. Paradoxically, ouabain was also reported to potentiate not only vasoconstriction but also vasodilation [9,57–59]. In our study, ouabain-induced elevation of blood pressure was associated with augmentation of total peripheral resistance, which was most pronounced in $\alpha_2^{+/G301R}$ mice. The major contribution of total peripheral resistance in this ouabain-induced blood pressure elevation was further supported by unaltered cardiac functions in both groups after ouabain administration. In line with previous ex vivo reports [9,57,60,61], our results suggest a primary pro-contractile action of ouabain on the vasculature at concentrations specific for α_2-isoform inhibition. We propose that reduction in the vascular expression of the α_2-isoform underlies the augmented ouabain-induced increase in total peripheral resistance in $\alpha_2^{+/G301R}$ mice. Accordingly, a similar concentration of circulating ouabain has a more efficient inhibitory action in $\alpha_2^{+/G301R}$ mice than in WT controls. Hence, our findings add to the perception of the importance of the α_2-isoform function for vascular tone and blood pressure in vivo in rodents as previously proposed [62,63].

Systolic time intervals entail information about the overall external myocardial efficiency [43]. The systolic time interval ratio increased only in $\alpha_2^{+/G301R}$ mice after ouabain administration suggesting a decrease in myocardial efficiency. This increase in the systolic

time interval ratio was a result of both a significant extension of the pre-ejection period and a slight shortening of the left ventricular ejection time. We suggest that the prolonged pre-ejection period may be a result of prolongation of the isovolumetric contraction phase of the heart as a result of the augmented ouabain-induced increase in total peripheral resistance in $\alpha_2^{+/G301R}$ mice [44]. However, we cannot exclude that ouabain induced changes in the electrical properties of the heart affecting the pre-ejection period [64], albeit heart rate was unchanged.

The inotropic effect of ouabain is well characterized, and it is described as a cardiac calcitrope, i.e., the inotropic effect is mediated by an increase in intracellular Ca^{2+} [27,65]. In our study, we assessed the arterial dP/dt_{max} as a proxy for cardiac contractility [41]. However, unlike the dP/dt_{max} measured directly in the left ventricle [66], the arterial dP/dt_{max} also depends on arterial system properties, e.g., the stiffness of the arterial wall [41]. In the current study, the arterial dP/dt_{max} was not affected following ouabain or vehicle administration during sinus rhythm. Considering that stroke volume and cardiac output did not change despite augmentation of total peripheral resistance in both WT and $\alpha_2^{+/G301R}$ mice, the presence of an inotropic effect of ouabain in our study during sinus rhythm is plausible. Additionally, shortening of left ventricular ejection time has been associated with an increase in intracellular Ca^{2+} mediated by cardiac calcitropes [43]. As left ventricular ejection time was only shortened in $\alpha_2^{+/G301R}$ mice, our finding may suggest a stronger cardiac effect of ouabain in $\alpha_2^{+/G301R}$ mice during sinus rhythm. In accordance, stroke volume and cardiac output were maintained in $\alpha_2^{+/G301R}$ mice despite greater augmentation of total peripheral resistance during sinus rhythm.

During atrial pacing, the arterial dP/dt_{max} was lower in $\alpha_2^{+/G301R}$ mice compared to WT after vehicle administration indicating a deleterious effect of time on the contractility in $\alpha_2^{+/G301R}$ mice. This was rescued by ouabain administration. However, the ouabain-induced recovery of arterial dP/dt_{max} in $\alpha_2^{+/G301R}$ mice compared to WT may also be a consequence of the augmented total peripheral resistance in $\alpha_2^{+/G301R}$ mice. In addition, the changes to systolic time intervals in $\alpha_2^{+/G301R}$ mice were not seen during atrial pacing. The systolic time intervals have been described to be influenced by heart rate, especially, in conjunction with hemodynamic changes [67–69]. Thus, in the current study, we suggest that the high heart rates (678 BPM) during atrial pacing compared to the heart rates during sinus rhythm (approximately 532 BPM) limits deviation of the systolic time intervals. This was further associated with reduced stroke volume in $\alpha_2^{+/G301R}$ mice. Thus, our findings may also suggest rate-dependent cardiac effects of ouabain.

Our study proposes a detrimental link between the vascular phenotype in $\alpha_2^{+/G301R}$ mice [9,10] and their cardiac function [11]. We suggest that the changes to cardiac function in $\alpha_2^{+/G301R}$ mice described in this study reflect the reduced ventricular function previously reported for aged $\alpha_2^{+/G301R}$ mice [11]. Furthermore, we suggest that the changed vascular reactivity, possibly in combination with intrinsic cardiac changes [11], underlies the pathological cardiovascular changes seen in $\alpha_2^{+/G301R}$ mice. This is based on the following observations from this and previous studies [9–11]: (i) the changed cardiac phenotype in $\alpha_2^{+/G301R}$ mice develops over time and is only seen in aged mice, (ii) the vascular phenotype in $\alpha_2^{+/G301R}$ mice is not unique to a specific age, and (iii) the presence of reduced cardiac efficiency in $\alpha_2^{+/G301R}$ mice when challenged with increments in afterload demonstrated in this study. However, whether parts of the cardiac changes are pre-defined or solely a product of the vascular abnormalities remain to be clarified. Nevertheless, all these aspects of cardiovascular dysfunction in $\alpha_2^{+/G301R}$ mice may in concert facilitate a milieu that leads to cardiac pathology over time [70]. Often, this type of cardiac disease progression is slow and silent, and it may resemble a heart failure phenotype with no apparent clinical symptoms during rest and sinus rhythm [71]. Similarly, the cardiac phenotype in $\alpha_2^{+/G301R}$ mice was only revealed during atrial pacing or after ouabain administration, and there was no apparent phenotype during sinus rhythm and at baseline in this study.

We primarily identified the changed cardiovascular phenotype in $\alpha_2^{+/G301R}$ mice. Intriguingly, the $\alpha_2^{+/G301R}$ mouse is also an animal model for migraine [21]. Migraine has been

described as a significant risk factor in the development of cardiovascular morbidity [72,73]. However, the underlying mechanism remains unclear. Studies have suggested that migraine may be considered a "channelopathy", specifically, that defects in ion transporters are the primary culprits in migraine pathology [74,75]. Furthermore, studies have argued that migraine should be considered a systemic disease rather than an isolated neurovascular condition [76,77]. Accordingly, our data suggest that global reduction of cardiovascular Na^+,K^+-ATPase α_2-isoform associated with the migraine-associated mutation changes the vascular phenotype with consequences for cardiac function in ${\alpha_2}^{+/G301R}$ mice. This notion warrants investigation of the cardiovascular phenotype of FHM2 migraineurs, which may further elucidate the molecular link between cardiovascular morbidity and migraine.

5. Conclusions

Our results indicate that both the cardiac and vascular phenotypes are affected in ${\alpha_2}^{+/G301R}$ mice in vivo. Our findings indicate less resilience of ${\alpha_2}^{+/G301R}$ hearts to the Na^+,K^+-ATPase α_2-isoform inhibition with ouabain. Specifically, ${\alpha_2}^{+/G301R}$ mice showed an augmented increase in total peripheral resistance associated with decreased cardiac efficiency in the presence of ouabain. We suggest that the hypercontractile vascular phenotype of the ${\alpha_2}^{+/G301R}$ mice may lead to detrimental cardiac function over time.

Supplementary Materials: The following supporting information can be downloaded at: https://www.mdpi.com/article/10.3390/biomedicines11020344/s1.

Author Contributions: Conceptualization, R.R., T.M.P., M.B.T., H.E.B. and V.V.M.; methodology, R.R., T.M.P., H.O.G., L.F.O. and V.V.M.; software, H.O.G.; validation, R.R., T.M.P., H.O.G. and L.F.O.; formal analysis, R.R., T.M.P., H.O.G., L.F.O. and V.V.M.; investigation, R.R. and L.F.O.; resources, V.V.M.; data curation, R.R. and V.V.M.; writing—original draft preparation, R.R. and V.V.M.; writing—review and editing, R.R., T.M.P., H.O.G., L.F.O., M.B.T., H.E.B. and V.V.M.; visualization, R.R. and H.O.G.; supervision, T.M.P., M.B.T., H.E.B. and V.V.M. project administration, V.V.M.; funding acquisition, V.V.M. All authors have read and agreed to the published version of the manuscript.

Funding: This research was funded by the Novo Nordisk Foundation, grant number NNF18OC0052021 and the Independent Research Fund Denmark, grant number 8020-00084B.

Institutional Review Board Statement: The animal study protocol was approved by the Animal Experiments Inspectorate of the Danish Ministry of Environment and Food (protocol code 2016-15-0201-00982, approved 23 June 2016; and protocol code 2021-15-0201-00986, approved 5 April 2022).

Informed Consent Statement: Not applicable.

Data Availability Statement: The datasets generated and analyzed during the current study are available from the corresponding author on reasonable request.

Acknowledgments: We thank Jane Holbæk Rønn and Viola Mose Larsen for the excellent technical assistance.

Conflicts of Interest: The authors declare no conflict of interest.

References

1. Skou, J.C. The influence of some cations on an adenosine triphosphatase from peripheral nerves. *Biochim. Biophys. Acta Bioenerg.* **1957**, *23*, 394–401. [CrossRef] [PubMed]
2. Clausen, M.V.; Hilbers, F.; Poulsen, H. The Structure and Function of the Na,K-ATPase Isoforms in Health and Disease. *Front. Physiol.* **2017**, *8*. [CrossRef]
3. Friedrich, T.; Tavraz, N.N.; Junghans, C. ATP1A2 Mutations in Migraine: Seeing through the Facets of an Ion Pump onto the Neurobiology of Disease. *Front. Physiol.* **2016**, *7*. [CrossRef]
4. Li, Z.; Langhans, S.A. Transcriptional regulators of Na,K-ATPase subunits. *Front. Cell Dev. Biol.* **2015**, *3*. [CrossRef] [PubMed]
5. Peng, M.; Huang, L.; Xie, Z.; Huang, W.H.; Askari, A. Partial inhibition of Na+/K+-ATPase by ouabain induces the Ca2+-dependent expressions of early-response genes in cardiac myocytes. *J. Biol. Chem.* **1996**, *271*, 10372–10378. [CrossRef] [PubMed]
6. Pratt, R.D.; Brickman, C.R.; Cottrill, C.L.; Shapiro, J.I.; Liu, J. The Na/K-ATPase Signaling: From Specific Ligands to General Reactive Oxygen Species. *Int. J. Mol. Sci.* **2018**, *19*, 2600. [CrossRef]

7. Mobasheri, A.; Avila, J.; Cózar-Castellano, I.; Brownleader, M.D.; Trevan, M.; Francis, M.J.; Lamb, J.F.; Martín-Vasallo, P. Na^+, K^+-ATPase isozyme diversity; comparative biochemistry and physiological implications of novel functional interactions. *Biosci. Rep.* **2000**, *20*, 51–91. [CrossRef]
8. Blanco, G.; Mercer, R.W. Isozymes of the Na-K-ATPase: Heterogeneity in structure, diversity in function. *Am. J. Physiol. Renal Physiol.* **1998**, *275*, F633–F650. [CrossRef]
9. Staehr, C.; Hangaard, L.; Bouzinova, E.V.; Kim, S.; Rajanathan, R.; Boegh Jessen, P.; Luque, N.; Xie, Z.; Lykke-Hartmann, K.; Sandow, S.L.; et al. Smooth muscle Ca2+ sensitization causes hypercontractility of middle cerebral arteries in mice bearing the familial hemiplegic migraine type 2 associated mutation. *J. Cereb. Blood Flow Metab.* **2019**, *39*, 1570–1587. [CrossRef]
10. Staehr, C.; Rajanathan, R.; Postnov, D.D.; Hangaard, L.; Bouzinova, E.V.; Lykke-Hartmann, K.; Bach, F.W.; Sandow, S.L.; Aalkjaer, C.; Matchkov, V.V. Abnormal neurovascular coupling as a cause of excess cerebral vasodilation in familial migraine. *Cardiovasc. Res.* **2019**, *116*, 2009–2020. [CrossRef]
11. Staehr, C.; Rohde, P.D.; Krarup, N.T.; Ringgaard, S.; Laustsen, C.; Johnsen, J.; Nielsen, R.; Beck, H.C.; Morth, J.P.; Lykke-Hartmann, K.; et al. Migraine Associated Mutation in the Na,K-ATPase Leads to Disturbances in Cardiac Metabolism and Reduced Cardiac Function. *J. Am. Heart Assoc.* **2022**, *11*, e021814. [CrossRef] [PubMed]
12. Bartlett, D.E.; Miller, R.B.; Thiesfeldt, S.; Lakhani, H.V.; Shapiro, J.I.; Sodhi, K. The Role of Na/K-ATPase Signaling in Oxidative Stress Related to Aging: Implications in Obesity and Cardiovascular Disease. *Int. J. Mol. Sci.* **2018**, *19*, 2139. [CrossRef]
13. Rindler, T.N.; Dostanic, I.; Lasko, V.M.; Nieman, M.L.; Neumann, J.C.; Lorenz, J.N.; Lingrel, J.B. Knockout of the Na,K-ATPase α_2-isoform in the cardiovascular system does not alter basal blood pressure but prevents ACTH-induced hypertension. *Am. J. Physiol.-Heart Circ. Physiol.* **2011**, *301*, H1396–H1404. [CrossRef]
14. Rindler, T.N.; Lasko, V.M.; Nieman, M.L.; Okada, M.; Lorenz, J.N.; Lingrel, J.B. Knockout of the Na,K-ATPase α2-isoform in cardiac myocytes delays pressure overload-induced cardiac dysfunction. *Am. J. Physiol.-Heart Circ. Physiol.* **2013**, *304*, H1147–H1158. [CrossRef]
15. Correll, R.N.; Eder, P.; Burr, A.R.; Despa, S.; Davis, J.; Bers, D.M.; Molkentin, J.D. Overexpression of the Na+/K+ ATPase α2 but not α1 isoform attenuates pathological cardiac hypertrophy and remodeling. *Circ. Res.* **2014**, *114*, 249–256. [CrossRef]
16. Shattock, M.J.; Ottolia, M.; Bers, D.M.; Blaustein, M.P.; Boguslavskyi, A.; Bossuyt, J.; Bridge, J.H.B.; Chen-Izu, Y.; Clancy, C.E.; Edwards, A.; et al. Na+/Ca2+ exchange and Na+/K+-ATPase in the heart. *Physiol. J.* **2015**, *593*, 1361–1382. [CrossRef]
17. Skogestad, J.; Aronsen, J.M. Regulation of Cardiac Contractility by the Alpha 2 Subunit of the Na+/K+-ATPase. *Front. Physiol.* **2022**, *13*. [CrossRef]
18. Pritchard, T.J.; Bowman, P.S.; Jefferson, A.; Tosun, M.; Lynch, R.M.; Paul, R.J. Na^+-K^+-ATPase and Ca^{2+} clearance proteins in smooth muscle: A functional unit. *Am. J. Physiol.-Heart Circ. Physiol.* **2010**, *299*, H548–H556. [CrossRef]
19. Pietrobon, D. Familial hemiplegic migraine. *Neurotherapeutics* **2007**, *4*, 274–284. [CrossRef]
20. Spadaro, M.; Ursu, S.; Lehmann-Horn, F.; Liana, V.; Giovanni, A.; Paola, G.; Frontali, M.; Jurkat-Rott, K. A G301R Na+/K+-ATPase mutation causes familial hemiplegic migraine type 2 with cerebellar signs. *Neurogenetics* **2004**, *5*, 177–185. [CrossRef]
21. Bøttger, P.; Glerup, S.; Gesslein, B.; Illarionova, N.B.; Isaksen, T.J.; Heuck, A.; Clausen, B.H.; Füchtbauer, E.M.; Gramsbergen, J.B.; Gunnarson, E.; et al. Glutamate-system defects behind psychiatric manifestations in a familial hemiplegic migraine type 2 disease-mutation mouse model. *Sci. Rep.* **2016**, *6*.
22. James, P.F.; Grupp, I.L.; Grupp, G.; Woo, A.L.; Askew, G.R.; Croyle, M.L.; Walsh, R.A.; Lingrel, J.B. Identification of a specific role for the Na,K-ATPase alpha 2 isoform as a regulator of calcium in the heart. *Mol. Cell.* **1999**, *3*, 555–563. [CrossRef]
23. Botelho, A.F.M.; Pierezan, F.; Soto-Blanco, B.; Melo, M.M. A review of cardiac glycosides: Structure, toxicokinetics, clinical signs, diagnosis and antineoplastic potential. *Toxicon* **2019**, *158*, 63–68. [CrossRef] [PubMed]
24. Pulgar, V.M.; Jeffers, A.B.; Rashad, H.M.; Diz, D.I.; Aileru, A.A. Increased constrictor tone induced by ouabain treatment in rats. *J. Cardiovasc. Pharmacol.* **2013**, *62*, 174–183. [CrossRef]
25. Li, M.; Martin, A.; Wen, C.; Turner, S.W.; Lewis, L.K.; Whitworth, J.A. Long-term ouabain administration does not alter blood pressure in conscious Sprague-Dawley rats. *Clin. Exp. Pharmacol. Physiol.* **1995**, *22*, 919–923. [CrossRef] [PubMed]
26. Cargnelli, G.; Trevisi, L.; Debetto, P.; Luciani, S.; Bova, S. Effect of long-term ouabain treatment on contractile responses of rat aortae. *J. Cardiovasc. Pharmacol.* **2000**, *35*, 538–542. [CrossRef] [PubMed]
27. Altamirano, J.; Li, Y.; DeSantiago, J.; Piacentino, V., 3rd; Houser, S.R.; Bers, D.M. The inotropic effect of cardioactive glycosides in ventricular myocytes requires Na+-Ca2+ exchanger function. *J. Physiol.* **2006**, *575*, 845–854. [CrossRef]
28. Obrien, W.J.; Lingrel, J.B.; Wallick, E.T. Ouabain Binding Kinetics of the Rat Alpha Two and Alpha Three Isoforms of the Sodium-Potassium Adenosine Triphosphate. *Arch. Biochem.* **1994**, *310*, 32–39. [CrossRef]
29. Yuan, C.M.; Manunta, P.; Hamlyn, J.M.; Chen, S.; Bohen, E.; Yeun, J.; Haddy, F.J.; Pamnani, M.B. Long-term ouabain administration produces hypertension in rats. *Hypertension.* **1993**, *22*, 178–187. [CrossRef]
30. Xavier, F.E.; Rossoni, L.V.; Alonso, M.J.; Balfagón, G.; Vassallo, D.V.; Salaices, M. Ouabain-induced hypertension alters the participation of endothelial factors in α-adrenergic responses differently in rat resistance and conductance mesenteric arteries. *Br. J. Pharmacol.* **2004**, *143*, 215–225. [CrossRef]
31. Shimoni, Y.; Gotsman, M.; Deutsch, J.; Kachalsky, S.; Lichtstein, D. Endogenous ouabain-like compound increases heart muscle contractility. *Nature* **1984**, *307*, 369–371. [CrossRef]
32. Simaan, J.; Fawaz, G.; Jarawan, S. The effect of ouabain-induced contractility on myocardial oxygen consumption. *Naunyn Schmiedebergs Arch. Pharmacol.* **1971**, *271*, 249–261. [CrossRef] [PubMed]

33. Rajanathan, R.; Pedersen, T.M.; Thomsen, M.B.; Botker, H.E.; Matchkov, V.V. Phenylephrine-Induced Cardiovascular Changes in the Anesthetized Mouse: An Integrated Assessment of in vivo Hemodynamics Under Conditions of Controlled Heart Rate. *Front. Physiol.* **2022**, *13*, 831724. [CrossRef] [PubMed]
34. Ikeda, K.; Onaka, T.; Yamakado, M.; Nakai, J.; Ishikawa, T.-o.; Taketo, M.M.; Kawakami, K. Degeneration of the Amygdala/Piriform Cortex and Enhanced Fear/Anxiety Behaviors in Sodium Pump α2 Subunit (Atp1a2)-Deficient Mice. *J. Neurosci.* **2003**, *23*, 4667–4676. [CrossRef]
35. Ikeda, K.; Onimaru, H.; Yamada, J.; Inoue, K.; Ueno, S.; Onaka, T.; Toyoda, H.; Arata, A.; Ishikawa, T.-o.; Taketo, M.M.; et al. Malfunction of Respiratory-Related Neuronal Activity in Na^+, K^+-ATPase α2 Subunit-Deficient Mice Is Attributable to Abnormal Cl^- Homeostasis in Brainstem Neurons. *J. Neurosci.* **2004**, *24*, 10693–10701. [CrossRef]
36. Percie du Sert, N.; Ahluwalia, A.; Alam, S.; Avey, M.T.; Baker, M.; Browne, W.J.; Clark, A.; Cuthill, I.C.; Dirnagl, U.; Emerson, M.; et al. Reporting animal research: Explanation and elaboration for the ARRIVE guidelines 2.0. *PLoS Biol.* **2020**, *18*, e3000411. [CrossRef] [PubMed]
37. Hauber, H.P.; Karp, D.; Goldmann, T.; Vollmer, E.; Zabel, P. Effect of low tidal volume ventilation on lung function and inflammation in mice. *BMC Pulm. Med.* **2010**, *10*, 21. [CrossRef] [PubMed]
38. Hansen, K.B.; Staehr, C.; Rohde, P.D.; Homilius, C.; Kim, S.; Nyegaard, M.; Matchkov, V.V.; Boedtkjer, E. PTPRG is an ischemia risk locus essential for HCO_3^--dependent regulation of endothelial function and tissue perfusion. *eLife* **2020**, *9*. [CrossRef]
39. Janssen, B.; Debets, J.; Leenders, P.; Smits, J. Chronic measurement of cardiac output in conscious mice. *Am. J. Physiol.-Regul. Integr. Comp. Physiol.* **2002**, *282*, R928–R935. [CrossRef]
40. Hill, L.K.; Sollers Iii, J.J.; Thayer, J.F. Resistance reconstructed estimation of total peripheral resistance from computationally derived cardiac output - biomed 2013. *Biomed. Sci. Instrum.* **2013**, *49*, 216–223.
41. Monge Garcia, M.I.; Jian, Z.; Settels, J.J.; Hunley, C.; Cecconi, M.; Hatib, F.; Pinsky, M.R. Performance comparison of ventricular and arterial dP/dtmax for assessing left ventricular systolic function during different experimental loading and contractile conditions. *Crit. Care* **2018**, *22*, 325. [CrossRef] [PubMed]
42. Cohn, P.F.; Liedtke, A.J.; Serur, J.; Sonnenblick, E.H.; Urschel, C.W. Maximal rate of pressure fall (peak negative dP/dt) during ventricular relaxation. *Cardiovasc. Res.* **1972**, *6*, 263–267. [CrossRef]
43. Alhakak, A.S.; Teerlink, J.R.; Lindenfeld, J.; Böhm, M.; Rosano, G.M.C.; Biering-Sørensen, T. The significance of left ventricular ejection time in heart failure with reduced ejection fraction. *Eur. J. Heart Fail.* **2021**, *23*, 541–551. [CrossRef] [PubMed]
44. Boudoulas, H. Systolic time intervals. *Eur. Heart J.* **1990**, *11 Suppl I*, 93–104. [CrossRef]
45. Vistisen, S.T.; Juhl-Olsen, P.; Frederiksen, C.A.; Kirkegaard, H. Variations in the pre-ejection period induced by deep breathing do not predict the hemodynamic response to early haemorrhage in healthy volunteers. *J. Clin. Monit. Comput.* **2014**, *28*, 233–241. [CrossRef] [PubMed]
46. Politi, M.T.; Ghigo, A.; Fernández, J.M.; Khelifa, I.; Gaudric, J.; Fullana, J.M.; Lagrée, P.-Y. The dicrotic notch analyzed by a numerical model. *Comput. Biol. Med.* **2016**, *72*, 54–64. [CrossRef]
47. National Center for Biotechnology Information. PubChem Compound Summary for CID 439501, O.R.J. 2022. Available online: https://pubchem.ncbi.nlm.nih.gov/compound/Ouabain (accessed on 18 January 2022).
48. Wittenberg, S.M. Chronotropic Effects of Ouabain and Heart Rate on Canine Atrium in Vivo. *Circ. Res.* **1974**, *34*, 258–267. [CrossRef] [PubMed]
49. Chiba, S.; Furukawa, Y.; Kobayashi, M. Direct positive chronotropic and inotropic effects of ouabain in the isolated and blood-perfused canine atrium. *Jpn. Heart J.* **1978**, *19*, 877–885. [CrossRef]
50. Salahudeen, M.S.; Nishtala, P.S. An overview of pharmacodynamic modelling, ligand-binding approach and its application in clinical practice. *Saudi. Pharm. J.* **2017**, *25*, 165–175. [CrossRef]
51. Matchkov, V.V.; Krivoi, I.I. Specialized Functional Diversity and Interactions of the Na,K-ATPase. *Front. Physiol.* **2016**, *7*, 179. [CrossRef]
52. Ferrandi, M.; Manunta, P.; Balzan, S.; Hamlyn, J.M.; Bianchi, G.; Ferrari, P. Ouabain-like Factor Quantification in Mammalian Tissues and Plasma. *Hypertension* **1997**, *30*, 886–896. [CrossRef]
53. Goto, A.; Yamada, K.; Nagoshi, H.; Terano, Y.; Omata, M. Stress-Induced Elevation of Ouabainlike Compound in Rat Plasma and Adrenal. *Hypertension* **1995**, *26*, 1173–1176. [CrossRef]
54. Bai, Y.-L.; Chu, Q.-J.; Li, J.; Chen, Y.-Y.; Li, W.-J.; Zhang, Q. A comparison of the effects of digoxin, ouabain and milrinone on naloxone-precipitated withdrawal syndrome in mice. *Eur. J. Pharmacol.* **2012**, *694*, 69–74. [CrossRef] [PubMed]
55. Yamazaki, T.; Akiyama, T.; Kitagawa, H.; Komaki, F.; Mori, H.; Kawada, T.; Sunagawa, K.; Sugimachi, M. Characterization of ouabain-induced noradrenaline and acetylcholine release from in situ cardiac autonomic nerve endings. *Acta Physiol.* **2007**, *191*, 275–284. [CrossRef]
56. Manunta, P.; Rogowski, A.C.; Hamilton, B.P.; Hamlyn, J.M. Ouabain-induced hypertension in the rat: Relationships among plasma and tissue ouabain and blood pressure. *J. Hypertens.* **1994**, *12*, 549–560. [CrossRef] [PubMed]
57. Cooke, J.P.; Shepherd, J.T.; Vanhoutte, P.M. Vasoconstriction induced by ouabain in the canine coronary artery: Contribution of adrenergic and nonadrenergic responses. *Cardiovasc. Drugs Ther.* **1988**, *2*, 255–263. [CrossRef] [PubMed]
58. Woolfson, R.G.; Hilton, P.J.; Poston, L. Effects of ouabain and low sodium on contractility of human resistance arteries. *Hypertension* **1990**, *15*, 583–590. [CrossRef] [PubMed]

59. Xie, J.; Wang, Y.; Summer, W.R.; Greenberg, S.S. Ouabain Enhances Basal Release of Nitric Oxide from Carotid Artery. *Am. J. Med. Sci.* **1993**, *305*, 157–163. [CrossRef]
60. Zhang, L.; Aalkjaer, C.; Matchkov, V.V. The Na,K-ATPase-Dependent Src Kinase Signaling Changes with Mesenteric Artery Diameter. *Int. J. Mol. Sci.* **2018**, *19*, 2489. [CrossRef]
61. Zulian, A.; Linde, C.I.; Pulina, M.V.; Baryshnikov, S.G.; Papparella, I.; Hamlyn, J.M.; Golovina, V.A. Activation of c-SRC underlies the differential effects of ouabain and digoxin on Ca(2+) signaling in arterial smooth muscle cells. *Am. J. Physiol. Cell Physiol.* **2013**, *304*, C324–C333. [CrossRef]
62. Zhang, J.; Lee, M.Y.; Cavalli, M.; Chen, L.; Berra-Romani, R.; Balke, C.W.; Bianchi, G.; Ferrari, P.; Hamlyn, J.M.; Iwamoto, T.; et al. Sodium pump α2 subunits control myogenic tone and blood pressure in mice. *Physiol. J.* **2005**, *569*, 243–256. [CrossRef] [PubMed]
63. Matchkov, V.V.; Moeller-Nielsen, N.; Dam, V.S.; Nourian, Z.; Briggs Boedtkjer, D.M.; Aalkjaer, C. The α2 isoform of the Na,K-pump is important for intercellular communication, agonist-induced contraction, and EDHF-like response in rat mesenteric arteries. *Am. J. Physiol.-Heart Circ. Physiol.* **2012**, *303*, H36–H46. [CrossRef] [PubMed]
64. Ruiz-Ceretti, E.; Samson, J.P.; Reisin, I.; Schanne, O.F. Ionic and electrical effects of quabain on isolated rabbit hearts. *J. Mol. Cell. Cardiol.* **1977**, *9*, 51–61. [CrossRef]
65. Psotka, M.A.; Gottlieb, S.S.; Francis, G.S.; Allen, L.A.; Teerlink, J.R.; Adams, K.F., Jr.; Rosano, G.M.C.; Lancellotti, P. Cardiac Calcitropes, Myotropes, and Mitotropes: JACC Review Topic of the Week. *J. Am. Coll. Cardiol.* **2019**, *73*, 2345–2353. [CrossRef] [PubMed]
66. Hamlin, R.L.; del Rio, C. dP/dtmax — A measure of 'baroinometry'. *J. Pharmacol. Toxicol. Methods* **2012**, *66*, 63–65. [CrossRef]
67. Warrington, S.J.; Weerasuriya, K.; Burgess, C.D. Correction of systolic time intervals for heart rate: A comparison of individual with population derived regression equations. *Br. J. Clin. Pharmacol.* **1988**, *26*, 155–165. [CrossRef]
68. Wolf, G.K.; Belz, G.G.; Stauch, M. Systolic time intervals—Correction for heart rate. *Basic Res. Cardiol.* **1978**, *73*, 85–96. [CrossRef]
69. Mertens, H.M.; Mannebach, H.; Trieb, G.; Gleichmann, U. Influence of heart rate on systolic time intervals: Effects of atrial pacing versus dynamic exercise. *Clin. Cardiol.* **1981**, *4*, 22–27. [CrossRef]
70. Ritterhoff, J.; Tian, R. Metabolism in cardiomyopathy: Every substrate matters. *Cardiovasc. Res.* **2017**, *113*, 411–421. [CrossRef]
71. Sabbah, H.N. Silent disease progression in clinically stable heart failure. *Eur. J. Heart Fail.* **2017**, *19*, 469–478. [CrossRef]
72. Hippisley-Cox, J.; Coupland, C.; Brindle, P. Development and validation of QRISK3 risk prediction algorithms to estimate future risk of cardiovascular disease: Prospective cohort study. *BMJ* **2017**, *357*, j2099. [CrossRef] [PubMed]
73. Adelborg, K.; Szépligeti, S.K.; Holland-Bill, L.; Ehrenstein, V.; Horváth-Puhó, E.; Henderson, V.W.; Sørensen, H.T. Migraine and risk of cardiovascular diseases: Danish population based matched cohort study. *BMJ* **2018**, *360*, k96. [CrossRef] [PubMed]
74. Sutherland, H.G.; Griffiths, L.R. Genetics of Migraine: Insights into the Molecular Basis of Migraine Disorders. *Headache J. Head Face Pain* **2017**, *57*, 537–569. [CrossRef]
75. Pellacani, S.; Sicca, F.; Di Lorenzo, C.; Grieco, G.S.; Valvo, G.; Cereda, C.; Rubegni, A.; Santorelli, F.M. The Revolution in Migraine Genetics: From Aching Channels Disorders to a Next-Generation Medicine. *Front. Cell. Neurosci.* **2016**, *10*, 156. [CrossRef] [PubMed]
76. Tietjen, G. Migraine as a Systemic Vasculopathy. *Cephalalgia* **2009**, *29*, 989–996. [CrossRef]
77. Venugopal, N.; Sriram Gopal, M.R. Migraine is a marker for systemic disease. *Indian J. Ophthalmol.* **2013**, *61*, 613. [CrossRef]

Disclaimer/Publisher's Note: The statements, opinions and data contained in all publications are solely those of the individual author(s) and contributor(s) and not of MDPI and/or the editor(s). MDPI and/or the editor(s) disclaim responsibility for any injury to people or property resulting from any ideas, methods, instructions or products referred to in the content.